

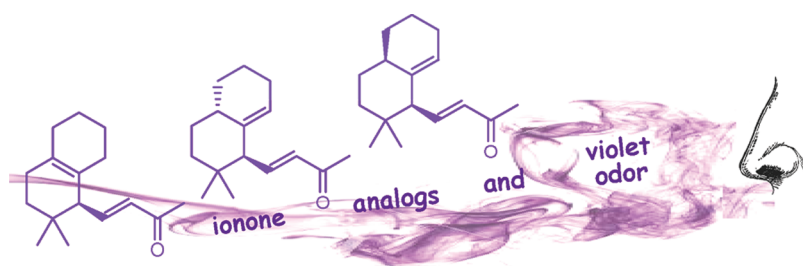
Enantioselective Synthesis and Olfactory Evaluation of Bicyclic α - and γ -Ionone Derivatives: The 3D Arrangement of Key Molecular Features Relevant to the Violet Odor of Ionones

Marco Luparia, Laura Legnani, Alessio Porta, Giuseppe Zanoni, Lucio Toma, and Giovanni Vidari*

Dipartimento di Chimica Organica, Università di Pavia, Via Taramelli 10, Pavia, Italy

vidari@unipv.it

Received July 12, 2009



Violet smelling ionones **1–3**, occurring in the headspace of different flowers, are well-known perfumery raw materials. With the goal to recognize the still ill-defined spatial arrangement of structural features relevant to the binding of ionones to olfactory G-protein coupled receptors, through B3LYP/6-31G(d) modeling studies we identified bicyclic compounds **7–9** as conformationally constrained 13-alkyl-substituted analogues of monocyclic α - and γ -ionones. They were thus synthesized to evaluate the olfactory properties. The enantioselective syntheses of **7–9** entailed two common key steps: (i) a Diels–Alder reaction to construct the octalinic core and (ii) a Julia–Lythgoe olefination to install the α,β -enone side chain. The odor thresholds of synthetic **7** and **9** were significantly lower than the corresponding parent ionones, and **9** showed the lowest threshold value among violet-smelling odorants examined so far. Modeling studies suggested a nearly identical spatial orientation of key hydrophobic and polar moieties of compounds **1**, **3**, and **4–9**. Presumably, interaction of these moieties with ionone olfactory receptors (ORs) triggers a similar receptor code that is ultimately interpreted by the human brain as a pleasant woody-violet smell. These results open the way to studies aimed at identifying and modeling complementary binding sites on α -helical domains of ionone receptor proteins.

Introduction

In the creation of violet and many other odor notes, α -, β -, and γ -ionones **1–3**, occurring in the headspace of different flowers in bloom, had constituted one of the most important groups of perfumery raw materials from the beginning of the perfumery industry, in the nineteenth century, until the present.¹ Indeed, the initially employed fabulously expensive natural odorants (violet flower absolute) have been replaced by cheap synthetic substitutes. Moreover, the search for new

odorants and floral notes, under the pressure of the increasing launch rates of perfumes, has often used the ionone structure as a source of inspiration leading to a plethora of different synthetic derivatives.^{2–7} These cover a broad range of odor notes from floral via animalic to woody

(1) Bauer, K.; Garbe, D.; Surburg, H. *Common Fragrance and Flavour Materials*, 4th ed.; Wiley–VCH: Weinheim, 2001.

(2) Chapuis, C.; Brauchli, R. *Helv. Chim. Acta* **1993**, *76*, 2070–2088.
 (3) Brenna, E.; Fuganti, C.; Serra, S. *Tetrahedron: Asymmetry* **2003**, *14*, 1–42.
 (4) Gautschi, M.; Bajgrowicz, J. A.; Kraft, P. *Chimia* **2001**, *55*, 379–387.
 (5) Sestanj, K. *Croat. Chem. Acta* **1962**, *34*, 211–217.
 (6) (a) Stoll, M.; Scherrer, W. *Helv. Chim. Acta* **1940**, *23*, 941–948. (b) Rouvé, A.; Stoll, M. *Helv. Chim. Acta* **1947**, *30*, 2216–2220.
 (7) (a) Kraft, P. *Synthesis* **1999**, 695–703. (b) Kraft, P.; Bajgrowicz, J. A.; Denis, C.; Fráter, G. *Angew. Chem., Int. Ed.* **2000**, *39*, 2980–3010.

characteristics, and a few possess greater intensity and superior lasting power (*substantivity*) than the parent ionones.⁴

A few years ago, we began a project on the synthesis of ionone derivatives aimed at obtaining new more efficient odorants and, at the same time, examining how humans are able to distinguish such compounds among so many odorant molecules. Our primary interest is to identify the still ill-defined spatial arrangement of molecular features encoding the violet odor, with the ultimate goal to design a general 3D model of the hydrophobic and polar groups relevant for the chemoreception of ionones. Indeed, we are well aware of the very complex mechanism underpinning the relationship between molecular structures and olfactory properties of odorants and on the difficulties of relating a given odor to a specific well-defined chemical structure.⁸ This fact is due to the complexity of the human olfactory system which encodes odor entities by using combinatorial coding schemes.⁹ Actually, the primary event of olfaction occurs in the olfactory epithelium where the odorant molecule can potentially interact with each of more than 390 different G-protein coupled olfactory receptors (ORs) expressed by active genes.¹⁰ Each receptor type responds to some odorant with greater intensity than to others, generating a pattern of receptor signaling which is transmitted to the human cortex through the olfactory nerve, where many gates along the pathway have the potential to shut off or enhance odor signals. Moreover, the olfactory signal pattern is integrated and combined in the brain with stimuli originated from the trigeminal nerve fibers and signals of other senses, chiefly the sense of taste, and so on.¹¹ Within this complex scenario, knowledge of the 3D geometries of molecules with well-established odor properties is of paramount importance to get insight into the binding modes with receptors of highest affinity, i.e., to identify complementary hydrophilic and lipophilic sections on α -helical domains of ORs stimulated at odorant threshold concentration.¹²

In this context, structure–odor relationships are more firmly established by examining the structural features of components of the same family, in which the contributions of different electronic, stereoelectronic, steric, and conformational properties of strictly related molecules are compared and distinguished more easily.¹³

Along this reasoning, in order to examine the influence of the C-5 alkyl substituent in the chemoreception of ionones,¹⁴ in previous studies we compared the olfactory properties of three synthetic 13-alkyl-substituted homologues 4–6 with parent (*S*)- α -ionone (1).¹⁵ It resulted that the three

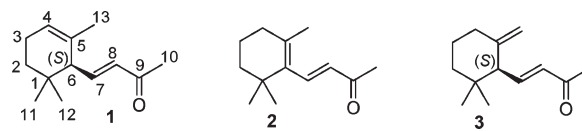


FIGURE 1. Structures of natural α -, β -, and γ -ionones (1–3).

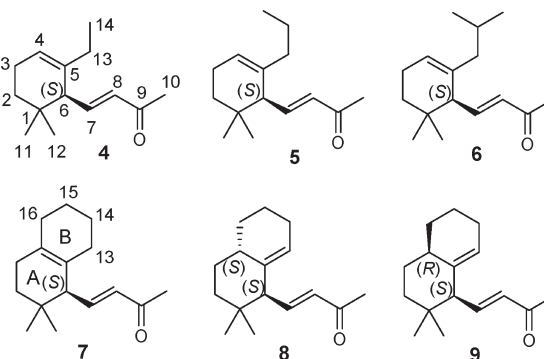


FIGURE 2. Structures of synthetic 13-alkyl-substituted α -ionones 4–6 and octalinic derivatives 7–9.

compounds maintained a predominant violet odor whose intensity dramatically depended on the steric hindrance of this group. Thus, the threshold of ionone 4 was more than 30 times lower than α -ionone 1, but larger alkyl groups derivatives showed minor odor potency.^{15a} Intrigued by these facts, we considered it of great interest to examine the olfactory properties of conformationally constrained synthetic 13-alkyl-substituted ionone analogues in which the alkyl residues were incorporated in a cyclic structure. Indeed, the rigidity of cyclic molecules generally precludes the range of steric profiles afforded by the multiple potential conformations of the more flexible, open-chained odorants, so that a more limited set of receptors are expected to be activated. In our case, this might allow us to define the active orientation of the 13-alkyl group in 4 with higher confidence and even lead to lower threshold odorants, should the conformationally constrained substituent give rise to a tighter binding with elicited olfactory receptor(s). Octalinic 7 was thus envisioned as a stiffened alkyl derivative of α -ionone (1), while the two diastereomers 8 and 9 were considered as conformationally constrained 13-alkyl-substituted analogues of γ -ionone (3). Actually, it was interesting to compare the geometry and odor properties of the α - and γ -octalinic series since there are significant differences between the conformational behavior and violet odor potency of α -ionone (1) and γ -ionone (3).^{15b}

Along this reasoning, at first the conformational spaces of target compounds 7–9 were explored; optimized conformations were then compared with those of 1, 3, and 4 in order to ascertain whether introduction of a fused ring would alter the spatial geometry of the parent monocyclic α - and γ -ionones. Modeling studies were followed by the enantioselective syntheses of the (*S*)-enantiomers of 7–9 along with the determination of their olfactory properties. Eventually, with all this information in hand, we could firmly define the spatial geometry of salient structural features associated with the violet-ionone odor, in particular the relative arrangement of relevant hydrophobic and polar binding sites of ionones to their ORs.

(8) Sell, C. S. *Angew. Chem., Int. Ed.* **2006**, *45*, 6254–6261.

(9) Malnic, B.; Hirono, J.; Sato, T.; Buck, L. B. *Cell* **1999**, *96*, 713–723.

(10) (a) Buck, L. B.; Axel, R. *Cell* **1991**, *65*, 175–187. (b) Axel, R. *Angew. Chem., Int. Ed.* **2005**, *44*, 6111–6127. (c) Buck, L. B. *Angew. Chem., Int. Ed.* **2005**, *44*, 6128–6140. (d) Zozulya, S.; Echeverri, F.; Nguyen, T. *Adv. Genome Biol.* **2001**, *2*, research 0018.1–0018.12; (e) Krautwurst, D. *Chem. Biodiv.* **2008**, *5*, 842–852.

(11) *The Chemistry of Fragrances*; Sell, C., Ed.; The Royal Society of Chemistry: Cambridge, 2006.

(12) Doszczak, L.; Kraft, P.; Weber, H.-P.; Bertermann, R.; Triller, A.; Hatt, H.; Tacke, R. *Angew. Chem., Int. Ed.* **2007**, *46*, 3367–3371.

(13) Other factors such as ligand volatility, solubility, and lipophilicity, as well as intrinsic entropic factors, are also important in determining the olfactory properties of compounds. They, however, should not vary significantly among structurally similar molecules.

(14) Jitkow, O. N.; Bogert, M. T. *J. Am. Chem. Soc.* **1941**, *63*, 1979–1984.

(15) (a) Luparia, M.; Boschetti, P.; Piccinini, F.; Porta, A.; Zannoni, G.; Vidari, G. *Chem. Biodivers.* **2008**, *5*, 1045–1057. (b) Legnani, L.; Luparia, M.; Zannoni, G.; Toma, L.; Vidari, G. *Eur. J. Org. Chem.* **2008**, 4755–4762.

Results and Discussion

Molecular Modeling of Bicyclic Ionones 7–9. The conformational space of compounds 7–9 was explored through optimization of all the possible starting geometries by the DFT approach at the B3LYP level with the 6-31G(d) basis set.¹⁶ All of the degrees of conformational freedom were considered, in particular the various possible conformations of the rings as well as the orientation of the butenone chain at C-6. Each octaline, independent from the position of the unconjugated double bond, presents 16 minimum energy conformations. The geometry of ring A and the consequent orientation of the butenone chain represent the main conformational feature of compounds 7–9; thus, the located conformations were collected in two groups of four families each, called A–D and E–H, respectively, differing in the geometry of ring A; in compound 7, this ring can assume two different half-chair conformations, whereas in compound 8, as well as in 9, it can assume a chair and a twisted-boat conformations, respectively (see below). Within each group, the four families differ from each other for the values of the torsion angles around the single bonds C-6–C-7 and C-8–C-9 of the butenone chain, each angle being associated with two energy minima. On the other hand, each family contains two members (a and b) differing for the two accessible puckering geometries of ring B. The most representative conformations of (6*S*)-configured compounds 7–9 are shown as 3D plots in Figures 3, 5, and 6, with each equilibrium percentage in parentheses.

Compound 7, the constrained analogue of α -ionones 1 and 4, parallels in all respects the conformational behavior of these two monocyclic ionones,^{15b} as shown by the very close values of the percentage contribution of each conformational family to the overall population (see Tables S1 and S2 in the Supporting Information). The torsional preferences of the butenone moiety are practically the same for the three compounds, as well as the preference of the A ring for the ²HC₁ geometry assumed by the A–D conformers (87.4%, 86.4%, and 85.9% for 7, 1, and 4, respectively). Thus, the pseudoaxial orientation of the side chain largely prevails over the pseudoequatorial one that is practically shown only by the E (9.8%, 10.5%, and 10.9% for 7, 1, and 4, respectively) and F members (2.7%, 3.0%, and 3.1%, respectively).

Figure 4 shows the superimpositions of 7Aa and 7Eb, the preferred ²HC₁ and ¹HC₂ geometries, respectively, of octaline 7 with the corresponding conformations 4A and 4E of compound 4 in which the ethyl group is *trans* oriented.^{15b} This comparison clearly shows that the presence of ring B, while freezing free rotations around the bond C-5–C-13 does not produce any distortion in the molecular shape of 7 with respect to 4, and it has no influence on the other degrees of conformational freedom.

For the diastereomeric bicyclic compounds 8 and 9 all of the geometries A–H could be located. However, additional constraints exerted by ring B changed dramatically the conformational mobility of ring A in comparison with parent γ -ionone 3. Actually, for compound 8, only the conformers A–D, in which ring A has the ⁴C₁ geometry

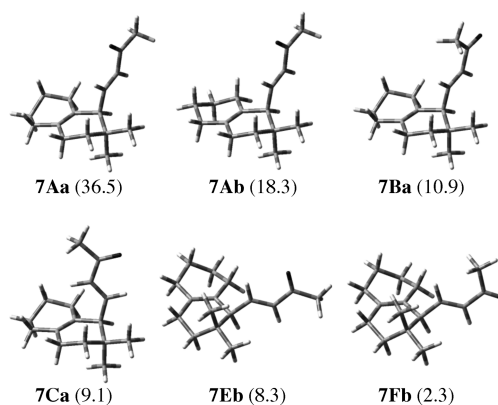


FIGURE 3. 3D-plot of the most representative conformations of compound 7.

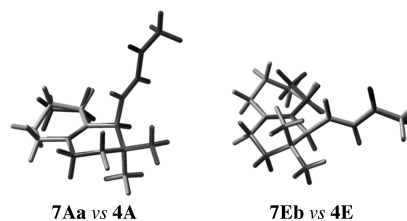


FIGURE 4. Overlap of the conformations 7Aa and 7Eb of compound 7 (gray shading) with the corresponding conformations of compound 4 (black shading), obtained through root-mean-square fitting of the atoms of ring A.

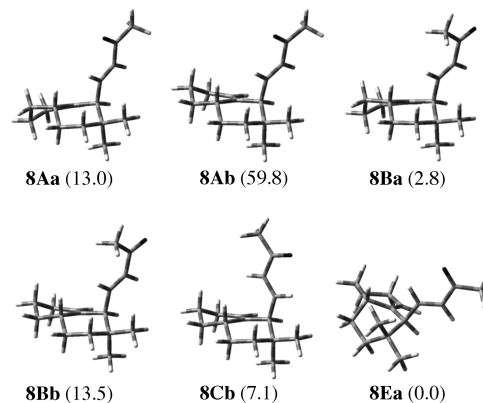


FIGURE 5. 3D-plot of representative conformations of compound 8.

and the butenone moiety is axially oriented, were populated (Figure 5), while geometries E–H made insignificant contributions to the conformational population. In striking contrast, diastereomer 9 almost exclusively exists in the E and F conformations, in which ring A has the ¹C₄ geometry and the side chain is equatorially oriented (Figure 6). A close examination of conformations E–H of compound 8 reveals the factors responsible for their high potential energy, which is about 5.6–8.0 kcal/mol above the lowest energy conformation 8Ab (Figure 5). In fact, fusion of ring B with ring A, in conjunction with the 4*S* stereocenter, prevents ring A from assuming the inverted ¹C₄ geometry typical of the E–H conformers of γ -ionone 3,^{15b} forcing it toward a boat geometry (see, for example, conformation 8Ea in Figure 5).

Conversely, for compound 9, analogous steric factors preclude ring A from adopting the typical ⁴C₁ geometry of

(16) (a) Becke, A. D. *J. Chem. Phys.* **1993**, *98*, 5648–5652. (b) Lee, C.; Yang, W.; Parr, R. G. *Phys. Rev. B* **1988**, *37*, 785–789.

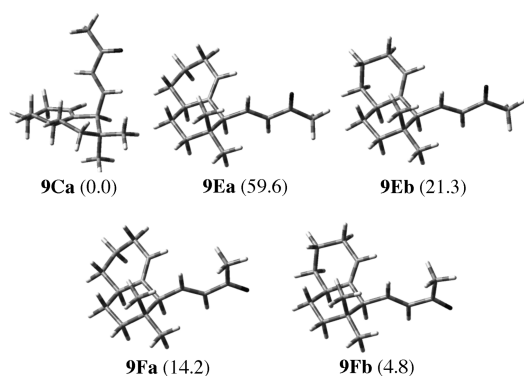


FIGURE 6. 3D-plot of representative conformations of compound 9.

conformers A–D, forcing the ring to assume a boat conformation (see, for example, conformation 9Ca in Figure 6). As a result, conformations A–D of compound 9 were calculated to be from about 6.8 to 12.3 kcal/mol less stable than the most populated one 9Ea. Moreover, it can be seen from Figures 5 and 6 that conformational changes occurring in ring B of compounds 8 and 9 do not cause appreciable distortions in ring A and have no influence on the other degrees of conformational freedom. Thus, it results clear that, disregarding the carbon chain C-14–C-16 in ring B, each of the ring A 4C_1 conformations 8A–D corresponds to the conformations A–D of γ -ionone 3, while each of the ring A 1C_4 conformations 9E–H corresponds to the conformations E–H of γ -ionone 3. Figure 7 shows, as examples, the nice overlaps of the most populated conformations of the two groups, namely 8Ab over 3A, and 9Ea over 3E.

On the basis of these findings we reasoned that odor evaluation of synthetic diastereomers 8 and 9 would allow a rough estimation of the contribution to the violet perfume of γ -ionone 3 of the two groups of conformations, namely those (A–D) with an axially oriented butenone chain and those (E–H) with an equatorially oriented side-chain.^{15b}

On the basis of the findings of the modeling studies, we decided to embark on the enantioselective synthesis of compounds 7–9.

Syntheses of Bicyclic Ionones 7–9. Diastereomers 8 and 9 were unreported in the literature; instead, enone 7 was previously prepared by phosphoric acid promoted cyclization of the corresponding pseudoionone precursor,¹⁷ which represents the classical synthetic access to ionones. Though this patented synthesis was short and rather efficient, compound 7 was obtained as a racemic mixture and contaminated by regioisomeric olefins. It is well-known that the regioisomer and enantiomer composition of ionones, as well as their chemical purity, greatly affect the olfactory properties in odor quality and thresholds. Therefore, although some odor characteristics of 7 have already been described,¹⁷ an innovative regio- and enantioselective approach to 7, as well to 8 and 9, was needed in order to collect more accurate olfactory data. (*S*)- α -Cyclogeraniol 10, readily obtained in 95% ee by lipase-mediated kinetic resolution of the racemate, was the common starting material.^{15a} The *S*-configuration corresponds to previously synthesized enantiomers 4–6,^{15a} as well as to the

(17) (a) Meuly, W. C.; Gradeff, P. S. Rhodia, Inc. U.S. Patent 3,480,677; *Chem. Abstr.* **1970**, 72, 21805t.

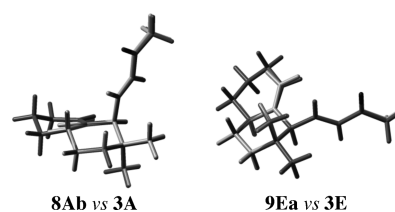
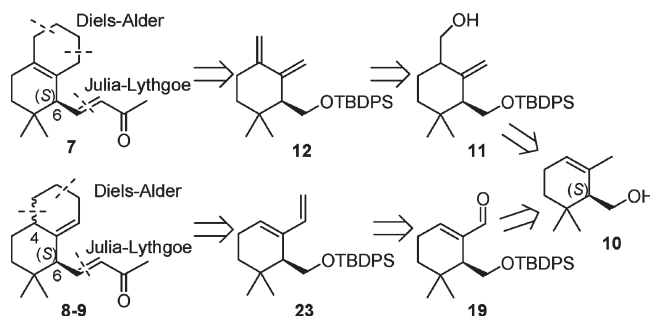


FIGURE 7. Overlap of the conformations 8Ab and 9Ea (black shading) of compounds 8 and 9, respectively, with the corresponding conformations of γ -ionone 3 (gray shading), obtained through root-mean-square fitting of the atoms of A ring.

SCHEME 1. Retrosynthetic Analysis of Target Compounds 7–9



more powerful antipode of natural ionones and related 2-methylionones (irones),³ with which the olfactory properties of 7–9 were compared. The envisioned routes to these compounds (Scheme 1) entailed two common key steps: (i) a Diels–Alder reaction to construct the unsaturated octalinic system and (ii) a Julia–Lythgoe olefination to install the α,β -enone side chain of the target compounds.

The latter olefination protocol was preferred to the more recent Julia–Kocienski variant on the basis of literature precedent¹⁸ and was anticipated to guarantee conservation of the stereochemical integrity at C-6 and complete (*E*)-stereoselectivity in the construction of the double bond in the side chain of products 7–9.^{15a} Notably, instead, the alternative Horner–Wadsworth–Emmons olefination of enantioenriched aldehyde α -cyclogeraniol, obtained by oxidation of alcohol 10,¹⁹ proceeded, at least in our hands, sluggishly and with erosion of the enantiomeric excess (ee) of product.²⁰ We observed a decrease of the ee even by following a special procedure suggested for the olefination of racemizable aldehydes under basic conditions.²¹ The bicyclic scaffolds of 7–9 were envisioned to arise from two Diels–Alder reactions between dienes 12 and 23, respectively, and a reactive electron-deficient ethene equivalent. Commercially available phenyl vinyl sulfone was the dienophile of choice since the electron-withdrawing sulfonyl group could be smoothly eliminated from the cycloaddition products.²² While the

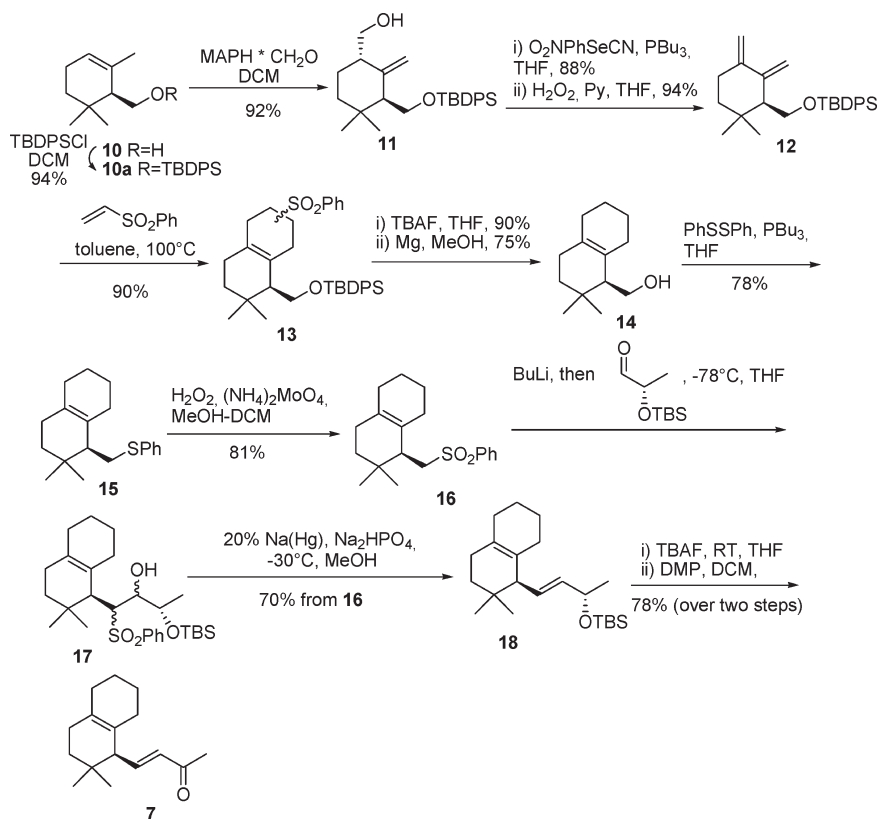
(18) Trost, B. M.; Shen, H. C.; Surivet, J. P. *J. Am. Chem. Soc.* **2004**, 126, 12565–12579.

(19) Mori, K.; Amaike, M.; Itou, M. *Tetrahedron* **1993**, 49, 1871–1878.

(20) Bovolenta, M.; Castronovo, F.; Vadalà, A.; Zanoni, G.; Vidari, G. *J. Org. Chem.* **2004**, 69, 8959–8962.

(21) Laval, G.; Audran, G.; Galano, J.-M.; Monti, H. *J. Org. Chem.* **2000**, 65, 3551–3554.

(22) (a) Carr, R. V. C.; Paquette, L. A. *J. Am. Chem. Soc.* **1980**, 102, 853–855. (b) Carr, R. V. C.; Williams, R. V.; Paquette, L. A. *J. Org. Chem.* **1983**, 48, 4976–1986. For some applications of this methodology in the field of natural products synthesis, see: (c) Omodani, T.; Shishido, K. *J. Chem. Soc., Chem. Commun.* **1994**, 2781–2782. (d) Devaux, J. F.; Hanna, I.; Lallemand, J. Y. *J. Org. Chem.* **1997**, 62, 5062–5068.

SCHEME 2. Total Synthesis of Octalinic α -Ionone 7

cycloaddition of diene **12** was expected to proceed uneventfully, the diastereoselectivity of the Diels–Alder reaction of diene **23** was rather unpredictable, though the bulky lateral substituent could, in principle, influence reagent approach. Regarding the preparation of dienes **12** and **23**, oxo-ene reaction (Prins reaction) of protected α -cyclogeraniol **10a** with formaldehyde,²³ followed by smooth dehydration of alcohol **11** seemed to be the fastest access to **12**, while olefination of aldehyde **19**, in principle achievable by allylic oxidation of **10a**, apparently provided the straightest approach to diene **23**.

At first, the synthesis of octalinic α -ionone **7** was pursued (Scheme 2). To this end, *O*-protected α -cyclogeraniol **10a** was subjected to Lewis acid catalyzed oxo-ene reaction with solid trioxane. In our first attempt, exposure of **10a** to Me_2AlCl (2.0 equiv) and trioxane (1.05 equiv) in CH_2Cl_2 from -78 to 0°C for 15 min²⁴ afforded the desired homoallylic alcohol **11** as a 4:1 mixture of *trans/cis* diastereomers in a moderate 50% combined yield. The low yield of this reaction was dramatically improved by substituting Me_2AlCl with the bulky Yamamoto reagent aluminum alkoxide methylaluminum bis(2,6-diphenylphenoxide) (MAPH).²⁵ By this means, the yield increased to 92% and

compound **11** was obtained as a single *trans*-diastereomer. This alcohol was then easily converted to the desired diene **12** according to Grieco's protocol.²⁶ Subsequently, our attention was directed to the crucial Diels–Alder reaction of diene **12** to produce a direct precursor of the key octalinic alcohol **14**. To this aim, heating compound **12** with phenyl vinyl sulfone in a sealed tube led to a clean formation of the expected mixture of regio- and diastereomeric cycloadducts **13** in almost quantitative yield.

These products converged to the desired free alcohol **14** after deprotection of the hydroxyl group followed by reductive elimination of the sulfonyl group. Having secured the bicyclic alcohol **14** by an efficient route, we submitted it to the Julia–Lythgoe olefination protocol²⁷ to install the enone moiety of target compound **7**. Accordingly, compound **14** was smoothly converted to the corresponding sulfide **15** under Mitsunobu conditions,²⁸ and the sulfide was chemoselectively oxidized to sulfone **16** with H_2O_2 and catalytic $(\text{NH}_4)_2\text{MoO}_4$.²⁹ Under these conditions, the cyclohexene double bond was not affected by the oxidant and the expected product was obtained in satisfactory overall yields. Subsequent addition of the anion derived from **16** to *O*-TBS-protected (*S*)-2-hydroxypropanal³⁰ proceeded uneventfully,

(23) For general reviews on the Prins and carbonyl ene reactions, see: (a) Snider, B. B. The Prins and Carbonyl Ene Reactions. In *Comprehensive Organic Synthesis*; Trost, B. M., Fleming, I., Semmelhack, M. F., Eds.; Pergamon Press: Oxford, 1991; Vol. 2, pp 527–561. (b) Mikami, K.; Shimizu, M. *Chem. Rev.* **1992**, *92*, 1021–1050.

(24) Cartaya–Marin, C. P.; Jackson, A. C.; Snider, B. B. *J. Org. Chem.* **1984**, *49*, 2443–2446.

(25) (a) Maruoka, K.; Concepcion, A. B.; Hirayama, N.; Yamamoto, H. *J. Am. Chem. Soc.* **1990**, *112*, 7422–7423. (b) Drake, D. J.; Jensen, R. S.; Busch-Petersen, J.; Kawakami, J. K.; Fernandez–Garcia, M. C.; Fan, P.; Makriyannis, A.; Tius, M. A. *J. Med. Chem.* **1998**, *41*, 3596–3608.

(26) Grieco, P. A.; Gilman, S.; Nishizawa, M. *J. Org. Chem.* **1976**, *41*, 1485–1486.

(27) Kocienski, P. J.; Lythgoe, B.; Ruston, S. *J. Chem. Soc., Perkin Trans. I* **1978**, 829–834.

(28) Ihara, M.; Suzuki, S.; Taniguchi, T.; Tokunaga, Y.; Fukumoto, K. *Tetrahedron* **1995**, *51*, 9873–9890.

(29) Schultz, H. S.; Freyermuth, H. B.; Buc, S. R. *J. Org. Chem.* **1963**, *28*, 1140–1142.

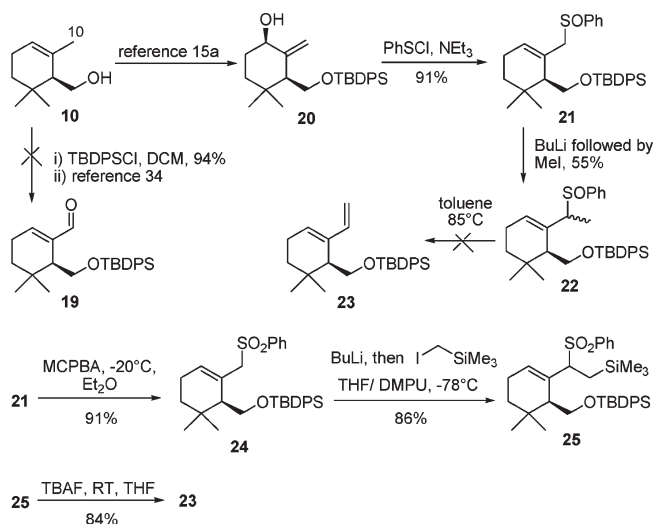
(30) Joly, G. D.; Jacobsen, E. N. *Org. Lett.* **2002**, *4*, 1795–1798.

with the exclusion of any Lewis acid catalyst.³¹ This contrasts significantly with the original procedure developed by Wicha for the coupling of lithiated sulfones with protected hydroxy aldehydes.³² The resulting β -hydroxy sulfone **17** was obtained as a mixture of diastereomers which, on exposure to 20% sodium amalgam, converged to protected ionol **18** in about 45% overall yield over four steps from alcohol **14**. The synthesis of enantiomerically enriched (*S*)-**7** (95% ee by chiral GC analysis), $[\alpha]_D^{20} = -295.3$ ($c = 1.3$, CH_2Cl_2), was completed in a straightforward manner by deprotection of **18**, followed by oxidation of the corresponding free allylic alcohol with the aid of Dess–Martin periodinane.³³

The syntheses of γ -ionone-type octalines **8** and **9** were more laborious than the preparation of the α -isomer **7**. On the basis of our original retrosynthetic strategy (Scheme 1), at first we concentrated our efforts toward the direct allylic oxidation of *O*-TBDPS-protected α -cyclogeraniol **14a** to aldehyde **19**. Although this transformation had been already described in the literature for a related substrate,³⁴ we were unable to reproduce this procedure for a clean oxidation of **10a**, obtaining, instead, a complex mixture of products. Therefore, we resorted to a more tortuous route in order to functionalize the C-10 position of compound **10**. This was based on conversion of **10** to allylic alcohol **20**,^{15a} followed by a Mislow–Evans [2,3]-sigmatropic rearrangement³⁵ of the corresponding sulfenate (Scheme 3). In the event, exposure of alcohol **20**^{15a} to PhSCl smoothly afforded sulfenoxide **21** as a mixture of diastereomers in 91% yield.

Alkylation of **21** readily gave the monomethyl product **22**, which was immediately submitted to thermal unimolecular elimination of PhSOH³⁶ with the expectation to obtain the desired diene **23**. Contrary to our hypothesis, compound **23** was produced only in poor yields, due to extensive decomposition. To avoid these problems, sulfenoxide **21** was oxidized to sulfone **24**, which was efficiently converted to diene **23** in three steps via TMS derivative **25**, according to the Kocienski procedure.³⁷ It must be stressed that the success of the alkylation of sulfone **24** strongly depended on the use of DMPU as cosolvent, since in THF alone the reaction afforded significantly lower yields. With diene **23** in hands, our attention was directed to the study of the crucial Diels–Alder reaction with phenyl vinyl sulfone (Scheme 4).²² In the event, the cycloaddition of **23** proceeded satisfactorily at a temperature significantly higher than that

SCHEME 3. Synthesis of Diene **28**



for the analogous Diels–Alder reaction of diene **12**, i.e., at 155 vs 100 °C. Furthermore, the addition of 10% w/w dihydroquinone was of paramount importance in order to obtain a clean reaction. As for the cycloaddition of diene **12**, the reaction of isomeric compound **23** afforded a mixture of different uncharacterized regio- and diastereomeric products, which were immediately submitted to cleavage of the silyl ether group and reductive removal of the sulfonyl group. The complex mixture of cycloadducts thus converged to a 55:45 mixture of only two diastereomeric alcohols, *trans*-**27** and *cis*-**28**, which were separated by careful flash column chromatography. The relative stereochemistry of these two compounds was established by means of extensive NMR experiments. The poor diastereoselectivity observed in the last Diels–Alder reaction clearly indicated that diastereotopic faces of diene **23** were nearly equally accessible by phenyl vinyl sulfone, the β -face being only slightly hindered by the bulky side arm. Subsequently, each of the two bicyclic alcohols **27** and **28** was separately converted uneventfully to the target compounds (*4S,6S*)-**8**, $[\alpha]_D^{20} = -10.4$ ($c = 1.5$, CH_2Cl_2), and **9**, $[\alpha]_D^{20} = -25.6$ ($c = 1.1$, CH_2Cl_2), according to two synthetic routes (Scheme 4) essentially identical to that previously described for isomeric α -ionone **7** (Scheme 2). Both compounds showed an ee of 95%.

Olfactory Evaluation of Bicyclic Ionones 7–9 and Alcohols 14, 27, and 28. Odor description and threshold values of the three bicyclic ionone homologues **7–9**, as well as the corresponding bicyclic alcohols **14, 27, and 28** (Givaudan Schweiz AG, Fragrance Research) are reported in Table 1. Experimental details of the olfactory evaluation are reported in the Supporting Information. Compared to the ionone derivatives, the odors of the three alcohols **14, 27, and 28** were significantly weaker and had no intense violet tonality, underlying the importance of a C-3-oxidized side chain in the chemoreception of ionones. Interestingly, the odor of bicyclic alcohol **28**, though not very powerful, displayed a very pleasant leathery note, with slightly meaty-animalic aspects, instead of floral-woody facets. As partly anticipated by the modeling studies, the three bicyclic isomers **7–9** maintained an intense violet ionone odor, but, in addition, each isomer showed individual pleasant characters, depending on the

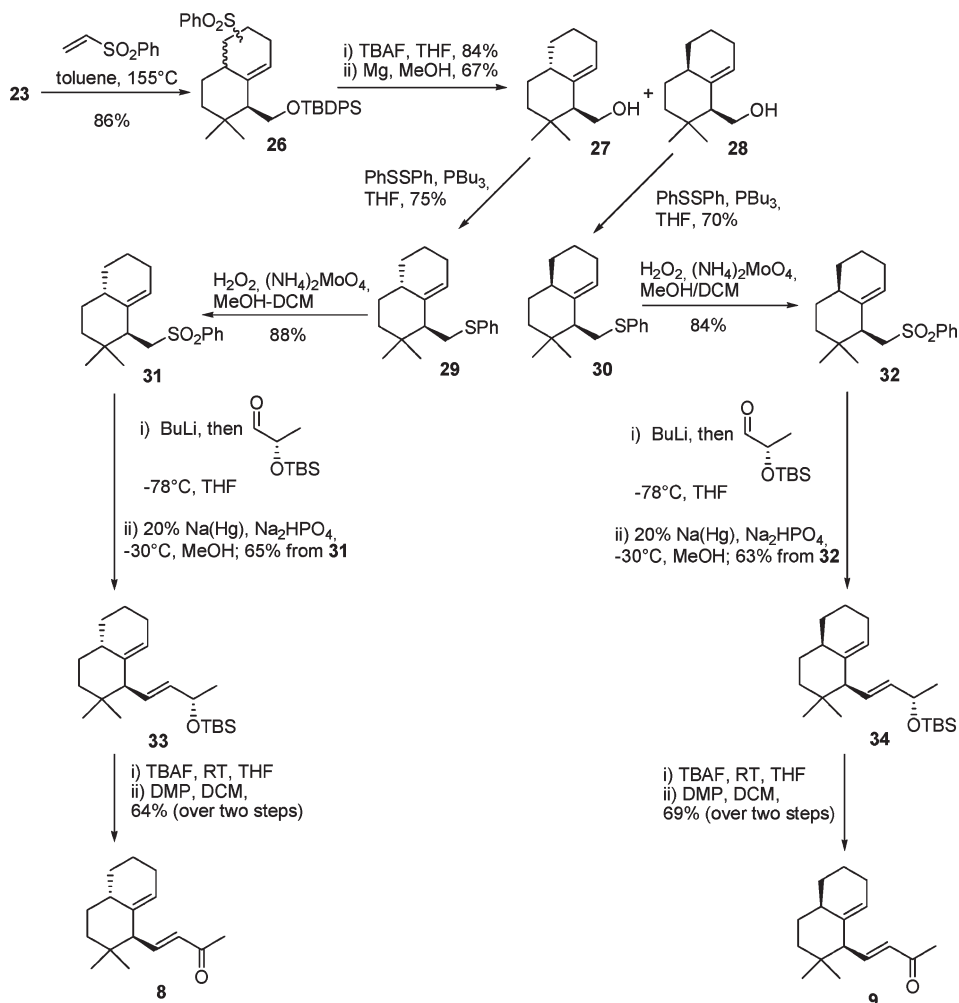
(31) Zanoni, G.; Porta, A.; Vidari, G. *J. Org. Chem.* **2002**, *67*, 4346–4351.
(32) Achmatowicz, B.; Baranowska, E.; Daniewski, A. R.; Pankowski, J.; Wicha, J. *Tetrahedron* **1988**, *44*, 4989–4998.

(33) Dess, D. B.; Martin, J. C. J. *Am. Chem. Soc.* **1991**, *113*, 7277–7287.
(34) (a) Wang, X.; Cui, Y.; Pan, X.; Chen, Y. *Bull. Soc. Chim. Belg.* **1995**, *104*, 563–565. (b) Wang, X.; Cui, Y.; Pan, X.; Chen, Y. *J. Indian Chem. Soc.* **1996**, *73*, 217–219.

(35) Altenbach, H.-J. Functional Group Transformations via Allyl Rearrangement. In *Comprehensive Organic Synthesis*; Trost, B. M., Fleming, I., Semmelhack, M. F., Eds.; Pergamon Press: Oxford, 1991; Vol. 6, pp 829–871.

(36) Krief, A. Alkylation of Sulfur and Selenium-containing Carbanions. In *Comprehensive Organic Synthesis*; Trost, B. M., Fleming, I., Semmelhack, M. F., Eds.; Pergamon Press: Oxford, 1991; Vol. 3, pp 85–191.

(37) (a) Kocienski, P. J. *Tetrahedron Lett.* **1979**, *20*, 2649–2650. For some examples of this methodology in multistep synthesis, see: (b) Kocienski, P. J. *J. Org. Chem.* **1980**, *45*, 2037–2039. (c) Hsiao, C. N.; Hannick, S. M. *Tetrahedron Lett.* **1990**, *31*, 6609–6612. (d) Kabat, M. M.; Wicha, J. *Tetrahedron Lett.* **1991**, *32*, 531–532. (e) Baldwin, J. E.; Adlington, R. M.; Bebbington, D.; Russell, A. T. *J. Chem. Soc., Chem. Commun.* **1992**, 1249–1251.

SCHEME 4. Conversion of Diene 23 to Octalinic γ -Ionones 8 and 9

position of the isolated double bond and the stereochemistry at C-4. Noticeably, in the context of odor–structure relationship, odor threshold of octalinic α -ionone derivative **7** was even slightly lower than the open-chained homologue **4**^{15a} (0.076 vs 0.085 ng/L), while odor characteristics were quite similar, including pronounced raspberry nuances. The nicely superimposable molecular shapes of the two compounds (Figure 4) strongly suggest that analogous steric and electronic factors are important in their chemoreception and that they activate a very close, or even an identical, pattern of ORs.

As for natural α - (**1**) and γ -ionone (**3**),³⁸ the γ -type octalinic isomer **9** was significantly more powerful than the corresponding α -type compound **7**; moreover, incorporation of the *exo* double bond of γ -ionone **3** inside the six-membered ring of compound **9** resulted in a lower odor threshold of almost 1 order of magnitude. *Actually, the odor threshold of compound 9 is the lowest among violet-smelling ionone derivatives evaluated so far.*

It is interesting to note that both diastereomers **8** and **9** display a violet–ionone odor (Table 1), irrespective of the opposite stereochemistry at C-4 and the inverted geometry of

ring A. However, the odor of compound **9**, in which the butenone chain is equatorially oriented (see the conformational studies above) is significantly stronger than **8**,³⁹ in which the side chain is axial. Given the nice overlaps of the **A–D** and **E–H** conformations of γ -ionone **3** with those of **8** and **9**, respectively (Figure 7), one can envisage that both types of conformers contribute to the violet odor of γ -ionone **3**, though the latter geometries allow for a tighter binding to OR(s). This conclusion is further confirmed by the diminution of odor threshold in the order **1** \rightarrow **3** \rightarrow **9**, which parallels a marked shift in the conformational equilibrium toward geometries of the equatorial type.^{15b}

At first sight, it appears rather unexpected that the two different conformations of γ -ionone **3** elicit an analogous violet odor perception, though with different potency; however, when properly oriented in space, several moieties of the two types of conformations can be brought to superimpose on each other quite nicely, as shown, for example, by comparing stereostructures **3E** and **3A**.^{15b} Thus, upon orienting and overlapping the two butenone side chains in a vertical plane, carbons C-1, C-2, C-5, C-6, C-11, and C-12 of **3E** can be brought to match with carbons C-1, C-12, C-5, C-

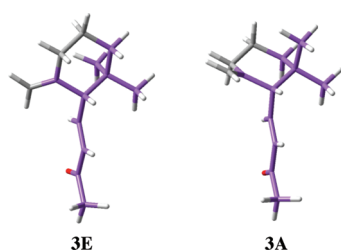
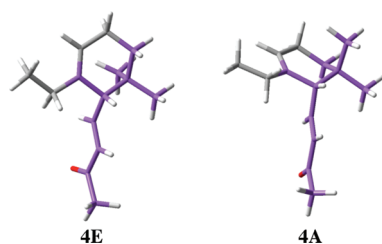
(38) Brenna, E.; Fuganti, C.; Serra, S.; Kraft, P. *Eur. J. Org. Chem.* **2002**, 967–978.

(39) Kraft, P.; Givaudan Schweiz A. G. Fragrance Research, personal communication.

TABLE 1. Odor Descriptions and Threshold Values of Compounds 7–9, 14, 27, and 28

product	odor description	threshold ^a
bicyclic alcohol 14	rather weak, fatty, wet cardboard odor with aromatic, thyme-like accents and slightly medicinal and mushroom-type nuances	undetermined
bicyclic alcohol 27	rather weak, sweet-powdery, fruity-woody, in the direction of ionone, with a bit of burnt aspects on top	undetermined
bicyclic alcohol 28	very pleasant, leathery note, with slightly meaty-animalic aspects and a slightly fatty nuance	37.9
bicyclic α -ionone 7	sweet, pleasant, fruity-woody ionone odor with a pronounced raspberry character; the finest of the three bicyclic ionones	0.076
bicyclic γ -ionone 8	fruity-woody ionone-odor, with spicy aspects of paprika	undetermined
bicyclic γ -ionone 9	dry, woody, pleasant ionone odor, with ambery and slightly medicinal aspects	0.010

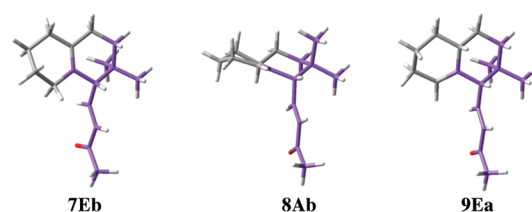
^aValues expressed as ng/L of air and determined by GC-olfactometry.

**FIGURE 8.** 3D-comparison of conformations **3E** and **3A** of γ -ionone **3**. Violet highlighted are the best overlapping moieties of the two conformations.**FIGURE 9.** 3D-comparison of conformations **4E** and **4A** of α -ionone derivative **4**. Violet highlighted are the best overlapping moieties of the two conformations.

6, C-2, and C-11 of **3A**, respectively (Figure 8). Instead, the sp^2 carbons C-13 result to be slightly tilted apart, while the ethylene moieties formed by carbons C-3 and C-4 lay in two orthogonal regions.

Actually, an analogous picture emerges for α -ionone **1** upon comparing conformations of types **1E** and **1A**.^{15b} In fact, in spite of the different geometries of the rings, the overall shape of **1E** is not very different from **3E**, as well as that of **1A** from **3A**,¹⁵ so that corresponding molecular moieties of each couple occupy nearly identical spatial regions. Extending the comparison to the preferred conformations of synthetic ionone derivatives **4** and **7–9**, similar 3D geometries can be recognized (Figures 9 and 10).

We thus assume that main binding of compounds **1** and **3–9** to ORs occurs through a similar spatial arrangement involving the atoms of the indicated overlapping moieties; instead, other molecular moieties and additional carbons are less critical for encoding the violet odor, though they possibly modulate the odor strength and introduce additional scent nuances.^{3,15a,38}

**FIGURE 10.** 3D-comparison of conformations **7Eb**, **8Ab**, and **9Ea** of octalinic ionones **7**, **8**, and **9**. Violet highlighted are the best overlapping moieties of the three conformations.

Conclusions

Discovered as early as 1893 by Tiemann and Krüger,⁴⁰ the ionones soon became central to the perfumery and fragrance chemistry. Although the design and synthesis of derivatives have provided some insights into the structure–odor relationship of violet odorants,^{5,7,14,15,41} a detailed study of the spatial arrangement of structural moieties relevant to the woody-violet odor of ionones was still lacking.

The B3LYP/6-31G(d) modeling studies and odor evaluation of compounds described herein suggest that the two main domains relevant for the violet smell, namely, the enone side chain and the alkyl groups near C-6 lay in almost orthogonal planes (see Figures 8–10) so that the carbonyl group is practically unhindered by the remaining part of the molecule, except for the adjacent methyl group. In addition, given the low energy barriers,⁴² the enone side chain can rotate rather freely around each of the two single bonds C-6–C-7 and C-8–C-9, thus easily assuming the best geometry to fit OR's binding sites. It is reasonable to assume that the acyl group, separated by two carbons from the lipophilic moiety, accepts a proton from an acidic group inside the receptor binding pocket. Indeed, a critical examination of the literature^{3,4,7b,43} shows that the carbonyl H-acceptor group is critical for violet odor since its substitution with other groups, for example,

(40) Tiemann, F.; Krüger, P. *Ber. Dtsch. Chem. Ges.* **1893**, *26*, 2675–2708.

(41) The relationship between molecular structure and violet odor has been interpreted by Turin with his controversial tunneling vibrational theory of olfaction: (a) Turin, L. *J. Theor. Biol.* **2002**, *216*, 367–385. (b) Keller, A.; Vosshall, L. B. *Nature Neurosci.* **2004**, *7*, 337–338.

(42) The energy profiles for rotation around the C(6)–C(7) and C(8)–C(9) bonds of conformations A and E of compounds **1**, **3**, and **4** were determined; the estimated rotation energy barriers resulted to be about 6–8 kcal/mol for both bonds of the three compounds.

(43) Leffingwell, J. C. Ionones, irones, damascones & structurally related odorants, found at http://www.leffingwell.com/chirality/ionone_iron.htm, 2009-08-22.

CH(OH)Me or CH(OAc)Me, results in differently smelling compounds.

As regards the geometry of the hydrophobic moieties, the alkyl groups of different ionone derivatives nearest C-6, *independently of the shape and conformation of the ring system*, can orient themselves in space to create a nearly identical hydrophobic environment at either sides of the enone unit (Figures 8–10). Instead, interactions with ORs pockets of alkyl groups residing in regions distant from C-6 are apparently less critical for encoding the violet odor.

The similar 3D geometry of prominent hydrophobic and polar sites with receptor(s) of highest affinity—see the violet-highlighted moieties in Figures 8–10—easily explains why ionone odorants with different structures, such as **1–3** and **4–9**, trigger a similar receptor code at the threshold concentration, generating an electrical signal ultimately interpreted by the higher human brain as a pleasant violet smell. We believe that this paper, having defined the 3D geometry of the molecular features relevant to olfactory chemoreception of ionones, will significantly contribute to studies aimed at modeling the binding sites of the G-protein-coupled receptors which they activate, a necessary step toward the understanding of the mechanism of the primary event involved in the perception/differentiation of the ionone odor. Furthermore, these studies have led to the finding of ionone odorants possessing the lowest odor thresholds known so far, namely compound **7** in the α -series and **9** in the γ -family, confirming the importance of molecular modeling and organic synthetic methods in the discovery of new potent odorous entities.

Experimental Section

[(1S,3S)-3-Hydroxymethyl-6,6-dimethyl-2-methylenecyclohexyl]-methanol *O*-tert-Butyldiphenylsilyl Ether (11**).** AlMe₃ (2.0 M in toluene, 5.4 mL, 10.7 mmol, 3 equiv) was added dropwise to a stirred solution of 2,6-diphenylphenol (5.28 g, 21.4 mmol, 6 equiv) in dry CH₂Cl₂ (71 mL) under Ar at rt. After 1 h of stirring, the reaction mixture was cooled to 0 °C, and then trioxane (370 mg, 4.1 mmol, 1.15 equiv) was added in one portion; the reaction was stirred for 1 h at 0 °C, and then compound **10a** (1.40 g, 3.6 mmol, 1 equiv) in CH₂Cl₂ (71 mL) was added via cannula. The reaction was stirred for 2 h, maintained at 0 °C, and then diluted with additional CH₂Cl₂ and poured into 1.2 M HCl. The aqueous layer was extracted with CH₂Cl₂, and the organic layer was washed with satd aq NaHCO₃, dried over MgSO₄, filtered, and concentrated under vacuum. The residue was purified by chromatography on silica gel (hexane/EtOAc 9/1) to give product **11** (1.39 g, 92%) as a colorless oil. $[\alpha]_D^{20} = +25.27$ ($c = 1.2$, CH₂Cl₂). IR (cm⁻¹) film: 3369, 3072, 2931, 2858, 1472, 1428, 1389, 1363, 1112, 889, 824, 740, 702, 614. ¹H NMR (300 MHz, CDCl₃): δ 7.70–7.63 (m, 4H), 7.47–7.35 (m, 6H), 4.89 (s, 1H), 4.85 (s, 1H), 3.88 (dd, $J = 5.1$, 10.4 Hz, 1H), 3.83–3.73 (m, 2H), 3.57 (dd, $J = 6.2$, 10.4, 1H), 2.27–2.15 (m, 1H), 2.11–2.04 (m, 1H), 1.75–1.65 (m, 1H), 1.43–1.23 (m, 4H), 1.04 (s, 9H), 0.85 (s, 3H), 0.81 (s, 3H). ¹³C NMR (75 MHz, CDCl₃): δ 148.0 (s), 135.8 (d), 134.1 (s), 129.7 (d), 127.8 (d), 110.2 (t), 64.4 (t), 62.4 (t), 55.5 (d), 43.0 (d), 36.0 (t), 34.4 (s), 28.7 (q), 27.0 (q), 25.9 (q), 25.9 (t), 19.4 (s). Anal. Calcd for C₂₇H₃₈O₂Si: C, 76.72; H, 9.06. Found: C, 76.88; H, 9.18.

[(S)-1,2,3,4,5,6,7,8-Octahydro-2,2-dimethylnaphthalen-1-yl]-methanol (14**): Representative Procedure for the Diels–Alder Reaction.** Diene **12** (553 mg, 1.4 mmol, 1 equiv) dissolved in dry toluene (2.6 mL) was treated with phenyl vinyl sulfone (276 mg, 1.64 mmol, 1.2 equiv) in a sealed tube under Ar. This mixture was heated for 24 h at 100 °C, and then the solvent was removed

under vacuum to afford crude sulfones **13**. This material was purified by FCC on silica gel (hexane/EtOAc 9/1) to yield a mixture of regio- and diastereomeric sulfones **13** (703 mg, 90%) as a white solid foam, which was immediately submitted to the subsequent step. To a stirred solution of sulfones **13** (1.41 g, 2.4 mmol, 1 equiv) in THF (24 mL) was added TBAF (1 M in THF, 4.9 mL, 2 equiv). The resulting mixture was stirred for 12 h, and then the solvent was removed under vacuum and the crude material was chromatographed on silica gel (hexane/EtOAc 7:3) to afford a mixture of regio- and diastereomeric hydroxy sulfones (741 mg, 90%). This mixture of alcohols (594 mg, 1.78 mmol, 1 equiv) was dissolved in HPLC-grade MeOH (25 mL) and treated with Mg turnings (432 mg, 10 equiv) at rt. After having been stirred vigorously until complete disappearance of starting material (TLC), the cloudy gray mixture was filtered, and the material remaining on the filter was washed with Et₂O. The filtrate was concentrated under controlled vacuum ($P > 90$ mmHg), diluted with Et₂O, and poured into satd aq NH₄Cl. The layers were separated, and the aqueous phase was extracted with Et₂O. The organic layer was dried over MgSO₄ and concentrated under controlled vacuum ($P > 90$ mmHg). The resulting residue was carefully separated by FCC on silica gel (pentane/Et₂O/CH₂Cl₂ 92:4:4) to afford alcohol **14** (259 mg, 75%) as a colorless pleasantly smelling oil. $[\alpha]_D^{20} = -47.6$ ($c = 1.4$, CH₂Cl₂). IR (cm⁻¹) film: 3368, 2924, 2832, 1448, 1386, 1364, 1062, 1014, 970. ¹H NMR (300 MHz, CDCl₃): δ 3.70 (br s, 2H), 2.16 (dd, $J = 1.9$, 18.5 Hz, 1H), 1.96–1.55 (m, 11H), 1.52 (br s, 1H), 1.27–1.10 (m, 1H), 1.00 (s, 3H), 0.87 ppm (s, 3H). ¹³C NMR (75 MHz, CDCl₃): δ 131.3 (s), 126.1 (s), 61.8 (t), 53.0 (d), 33.2 (t), 32.0 (s), 30.5 (t), 29.6 (t), 28.4 (t), 28.1 (q), 27.9 (q), 23.6 (t), 23.4 (t). Anal. Calcd for C₁₃H₂₂O: C, 80.35; H, 11.41. Found: C, 80.47; H, 11.51.

[(S)-1,2,3,4,5,6,7,8-Octahydro-2,2-dimethylnaphthalen-1-yl]-methyl(phenyl)sulfane (15**): Representative Procedure for Alcohol to Sulfide Conversion.** To a stirred solution of alcohol **14** (191 mg, 0.98 mmol, 1 equiv) in dry THF was added PhSSPh (537 mg, 2.5 mmol, 2.5 equiv), followed by the dropwise addition of PBu₃ (607 μ L, 2.5 mmol, 2.5 equiv) under Ar at rt. The mixture was stirred for 5 h, and then additional PhSSPh (322 mg, 1 equiv) followed by PBu₃ (364 μ L, 1 equiv) were added. The reaction was stirred at rt for an additional 4 h and diluted with Et₂O and H₂O. The layers were separated, and the aqueous phase was extracted with Et₂O. The combined organic extracts were dried over MgSO₄, and the solvent was removed under vacuum to afford a residue which was separated on reversed phase (RP-18, MeOH/H₂O 94:6) to give sulfide **15** (219 mg, 78%) as a pale yellow oil. $[\alpha]_D^{20} = -105.1$ ($c = 1.6$, CH₂Cl₂). IR (cm⁻¹) film: 3059, 2925, 2832, 1586, 1480, 1438, 1385, 1364, 1090, 1026. ¹H NMR (300 MHz, CDCl₃): δ 7.38–7.25 (m, 4H), 7.20–7.13 (m, 1H), 3.07 (dd, $J = 6.0$, 12.3 Hz, 1H), 2.90 (dd, $J = 3.4$, 12.3 Hz, 1H), 2.15 (br d, $J = 18.5$ Hz, 1H), 1.94–1.51 (m, 11H), 1.29–1.19 (m, 1H), 1.04 (s, 3H), 0.91 (s, 3H). ¹³C NMR (75 MHz, CDCl₃): δ 138.7 (s), 129.4 (s), 129.0 (d), 128.9 (d), 128.0 (s), 125.6 (d), 50.0 (d), 35.7 (t), 32.7 (s), 32.1 (t), 30.4 (t), 29.9 (t), 28.4 (t), 28.1 (q), 27.4 (q), 23.6 (t), 23.3 (t). Anal. Calcd for C₁₉H₂₆S: C, 79.66; H, 9.15. Found: C, 79.88; H, 9.25.

(S)-1,2,3,4,5,6,7,8-Octahydro-2,2-dimethyl-1-[(phenylsulfonyl)-methyl]naphthalene (16**): Representative Procedure of Sulfide Oxidation.** Sulfide **15** (250 mg, 0.87 mmol, 1 equiv) was dissolved in MeOH (9.6 mL) and CH₂Cl₂ (0.64 mL), and then (NH₄)₂MoO₄ (75 mg, 30% in weight with respect to the sulfide) and H₂O₂ (1.0 mL, 35% solution) were added at rt. After 12 h of stirring, the reaction was quenched by the addition of solid Na₂SO₃ and allowed to stir for 20 min. The resulting heterogeneous mixture was filtered, and the solvent was evaporated under vacuum. The residue was partitioned between CH₂Cl₂ and semisatd aq NH₄Cl. The phases were separated, and the aqueous layer was extracted

with CH₂Cl₂. Combined organic layers were dried over MgSO₄ and concentrated under vacuum. The crude material was purified by flash column chromatography (hexane/EtOAc 93:7) to yield sulfone **16** (226 mg, 81%) as a white solid. $[\alpha]_D^{20} = -62.0$ ($c = 1.0$, CH₂Cl₂). IR (cm⁻¹) film: 3065, 2923, 2833, 1447, 1302, 1151, 1087, 783, 755, 740. ¹H NMR (300 MHz, CDCl₃): δ 7.96–7.89 (m, 2H), 7.68–7.51 (m, 3H), 3.22 (dd, $J = 4.5, 15.1$ Hz, 1H), 2.88 (dd, $J = 3.3, 15.1$ Hz, 1H), 2.17 (br s, 1H), 2.05 (br d, 17 Hz, 1H), 2.00–1.42 (m, 10H), 1.32–1.15 (m, 1H), 0.90 (2 overlapped s, totally 6H). ¹³C NMR (75 MHz, CDCl₃): δ 140.7 (s), 133.6 (d), 129.5 (s), 129.4 (d), 128.2 (d), 59.3 (t), 43.6 (d), 32.4 (s), 31.9 (t), 30.3 (t), 28.9 (t), 28.3 (t), 27.6 (q), 26.3 (q), 23.5 (t), 23.1 (t). Anal. Calcd for C₁₉H₂₆O₂S: C, 71.66; H, 8.23. Found: C, 71.83; H, 8.34.

(3S,E)-4-[(S)-1,2,3,4,5,6,7,8-Octahydro-2,2-dimethylnaphthalen-1-yl]but-3-en-2-ol O-TBS Ether (18): Representative Procedure of Julia–Lythgoe Olefination. *n*-BuLi (1.6 M in hexane, 488 μ L, 0.78 mmol, 1.1 equiv) was added dropwise to a cold (–78 °C) solution of sulfone **16** (226 mg, 1 equiv) in dry THF (7.1 mL) under Ar. The resulting yellow mixture was stirred at –78 °C for 30 min, and then aldehyde (*S*)-MeCH(*O*-TBS)CHO³⁰ (154 mg, 0.82 mmol, 1.15 equiv) in THF (2 mL) was added via cannula. The reaction was stirred for 90 min at –78 °C and then was diluted with Et₂O and quenched with satd aq NH₄Cl. The layers were separated, and the aqueous phase was extracted with Et₂O. The combined organic layers were washed with brine, dried over MgSO₄, and concentrated under vacuum affording crude **17**. This residue was dissolved in HPLC-grade MeOH (24.6 mL), cooled to –30 °C, and treated with Na₂HPO₄ (2.45 g) and 20% Na/Hg alloy (1.04 g). After 1 h at –30 °C, the reaction mixture was filtered, and the solvent was removed under vacuum at ≥ 60 mmHg. The resulting crude oil was dissolved in CH₂Cl₂ and washed with satd aq NH₄Cl. The aqueous layer was extracted with CH₂Cl₂, and the combined organic extracts were dried over MgSO₄ and concentrated under vacuum. The crude product was purified by FCC on silica gel (hexane) to afford product **18** (175 mg, 70% from **16**) as a white oil. $[\alpha]_D^{20} = -167.0$ ($c = 1.8$, CH₂Cl₂). IR (cm⁻¹) film: 2927, 1472, 1362, 1254, 1147, 1080, 1004, 834, 775, 665. ¹H NMR (300 MHz, CDCl₃): δ 5.48–5.26 (m, 2H), 4.27 (distorted quint, J about 6.2 Hz, 1H), 1.99 (d, $J = 7.3$ Hz, 1H), 1.90–1.77 (m, 5H), 1.70–1.39 (m, 6H), 1.22 (d, $J = 6.3$ Hz, 3H), 1.27–1.12 (m, 1H), 0.89 (s, 9H), 0.87 (s, 3H), 0.80 (s, 3H), 0.05 (s, 3H), 0.04 (s, 3H). ¹³C NMR (75 MHz, CDCl₃): δ 136.3 (d), 130.1 (d), 128.5 (s), 127.4 (s), 69.9 (d), 54.3 (d), 32.5 (t), 32.3 (s), 30.4 (t), 29.3 (t), 28.5 (t), 27.6 (q), 27.2 (q), 26.0 (q), 25.3 (q), 23.6 (t), 23.4 (t), 18.5 (s), –4.4 (q), –4.6 (q). Anal. Calcd for C₂₂H₄₀O₂Si: C, 75.79; H, 11.56. Found: C, 75.92; H, 11.72.

(3E)-4-[(S)-1,2,3,4,5,6,7,8-Octahydro-2,2-dimethylnaphthalen-1-yl]but-3-en-2-one (7): Representative Procedure of Allylic Alcohol Oxidation. Crude alcohol obtained by standard deprotection of **18** (see the Supplementing Information) (0.5 mmol, slightly contaminated by TBSF) was dissolved in dry CH₂Cl₂ (5 mL) and treated with DMP (255 mg, 0.5 mmol, 1 equiv) at rt. After being stirred for 1 h, the mixture was diluted with CH₂Cl₂ and poured into satd aq NaHCO₃ and Na₂S₂O₃. The layers were separated, and the aqueous phase was extracted with CH₂Cl₂. The combined organic layers were dried over MgSO₄, filtered, and concentrated at $P > 200$ mmHg. The crude product was purified by FCC on silica gel (pentane/Et₂O 98/2) to afford the desired α,β -unsaturated ketone **7** (91 mg, 78% yield over two steps) as a colorless pleasant-smelling oil. ee = 95% determined by chiral GC with the following temperature program: 80 °C (3 min) \rightarrow 1°/min \rightarrow 130 °C (40 min) \rightarrow 2°/min \rightarrow 170 °C (0 min) \rightarrow 4°/min \rightarrow 200 °C (4 min). (–)-**7**: t_R 106.3. (+)-**7**: t_R 106.8. $[\alpha]_D^{20} = -295.3$ ($c = 1.3$, CH₂Cl₂). IR (cm⁻¹) film: 2924, 2884, 1697, 1675, 1618, 1446, 1363, 1252, 992, 738. ¹H NMR (300 MHz, CD₂Cl₂): δ 6.62 (dd, $J = 9.7, 15.8$ Hz, 1H), 6.01 (br d, $J = 15.8$ Hz, 1H), 2.24 (s, 3H), 2.23 (d, $J = 9.7$ Hz, 1H), 2.01–1.85 (m, 5H), 1.74–1.51 (m, 6H), 1.35–1.23 (m, 1H), 0.95 (s, 3H), 0.87 (s, 3H). ¹³C NMR (75 MHz, CD₂Cl₂): δ 198.5 (s), 149.8 (d), 132.4 (d), 129.7 (s), 126.6

(s), 55.2 (d), 32.8 (s), 32.3 (t), 30.6 (t), 29.6 (t), 28.6 (t), 27.9 (q), 27.0 (q), 26.9 (q), 23.7 (t), 23.5 (t). Anal. Calcd for C₁₆H₂₄O: C, 82.70; H, 10.41. Found: C, 82.83; H, 10.35.

[(S)-6,6-Dimethyl-2-[(phenylsulfinyl)methyl]cyclohex-2-enyl]methanol O-tert-Butyldiphenylsilyl Ether (21). Phenylthiol (2.15 mL, 21.0 mmol, 2 equiv) was added dropwise to a stirred solution of *N*-chlorosuccinimide (2.8 g, 21.0 mmol, 2 equiv) in dry toluene (77.5 mL) at 0 °C under Ar. The mixture was then stirred at rt for 1 h, during which time it became orange-yellow with a white precipitate.⁴⁴ A 58 mL portion of the supernatant toluene solution of PhSCl (1.5 equiv) was slowly added with a gas-tight syringe to a stirred solution of allylic alcohol **20**^{15a} (4.28 g, 10.5 mmol) in dry NEt₃ (15 mL) at rt under Ar. The yellow-orange solution of PhSCl discolored immediately, and the reaction mixture became a white slurry. After 1 h, the mixture was diluted with Et₂O and H₂O. The layers were separated, and the aqueous phase was extracted with Et₂O. The combined organic layers were dried over MgSO₄, filtered, and concentrated under vacuum to give a crude oil which was purified by FCC on silica gel (from hexane/EtOAc 85:15 to 4:1). Sulfoxide **21** (4.91 g, 91%, mixture of diastereomers) was obtained as a pale yellow oil. IR (cm⁻¹) film: 3070, 2957, 2929, 2856, 1472, 1443, 1427, 1112, 1086, 1049, 998, 823, 745, 702, 613. ¹H NMR (300 MHz, CDCl₃): δ 7.75–7.28 (m, 15H), 5.80 and 5.48 (2 br s, 1H overall), 3.82–3.63 (m, 2H), 3.59–3.17 (m, 2H), 2.25–1.50 (m, 4H), 1.25–1.12 (m, 1H), 1.01 (2s, 9H), 0.96, 0.93, 0.85 (3s, 6H overall). Anal. Calcd for C₃₂H₄₀O₂SSi: C, 74.37; H, 7.80. Found: C, 74.48; H, 7.91.

[(S)-6,6-Dimethyl-2-[(trimethylsilyl)-1-(phenylsulfonyl)ethyl]cyclohex-2-enyl]methanol O-tert-Butyldiphenylsilyl Ether (25). To a cold (–78 °C) stirred solution of sulfone **24** (4.02 g, 7.5 mmol, 1 equiv) in dry THF (75.4 mL) under Ar was added DMPU (1.8 mL, 15.0 mmol, 2 equiv) followed by dropwise addition of BuLi (1.6 M in hexane, 5.4 mL, 8.7 mmol, 1.15 equiv). The resultant yellow solution was left at –78 °C for 20 min, and then ICH₂SiMe₃ (1.3 mL, 8.7 mmol, 1.15 equiv) was added. After having been stirred for 1 h at –78 °C, the mixture was diluted with Et₂O and quenched by addition of satd aq NH₄Cl. The layers were separated and the aq. phase was extracted with Et₂O. The combined organic extracts were dried over Na₂SO₄ and concentrated in vacuo. The crude oil was chromatographed on silica gel (hexane/EtOAc 95:5) to provide TMS-sulfone **25** (86%) as a pale yellow oil. IR (cm⁻¹) film: 3071, 2956, 1472, 1447, 1428, 1305, 1265, 1249, 1143, 1112, 1084, 856, 824, 803, 737, 703, 615. ¹H NMR (300 MHz, CDCl₃): δ 7.78–7.27 (m, 15H), 6.19 (br s, 1H), 4.15–4.12 (dd, $J = 6.6, 8.5$ Hz, 1H), 3.81 (dd, $J = 5.3, 11.4$ Hz, 1H), 3.54 (dd, $J = 5.0, 11.4$ Hz, 1H), 2.18–1.97 (m, 3H), 1.35–1.20 (m, 4H), 1.10 (s, 9H), 0.87 (s, 3H), 0.85 (s, 3H), 0.02 (s, 9H). ¹³C NMR (75 MHz, CDCl₃): δ 138.5 (s), 135.8 (d), 133.9 (s), 133.7 (s), 133.0 (d), 132.1 (s), 131.1 (d), 129.9 (d), 129.8 (d), 129.4 (d), 128.6 (d), 127.9 (d), 127.7 (d), 64.3 (d), 63.4 (t), 51.9 (d), 34.5 (t), 32.4 (s), 28.8 (q), 27.1 (q), 24.3 (q), 23.2 (t), 20.2 (t), 19.2 (s), –0.4 (q). Anal. Calcd for C₃₆H₅₀O₃SSi₂: C, 69.85; H, 8.14. Found: C, 70.02; H, 8.27.

[(S)-6,6-Dimethyl-2-vinylcyclohex-2-enyl]methanol O-tert-Butyldiphenylsilyl Ether (23). TBAF (1 M in THF, 18.2 mL, 18.2 mmol, 2.5 equiv) was added to a stirred solution of **25** (4.51 g, 7.3 mmol, 1 equiv) in dry THF (15 mL) at rt. The reaction mixture was stirred for 40 min, followed by dilution with Et₂O and H₂O. The layers were separated, and the aqueous phase was extracted with Et₂O. The combined organic extracts were dried over Na₂SO₄ and concentrated under vacuum. The crude material was purified by FCC on silica gel (hexane) to provide diene **23** (2.48 g, 84%) as a colorless oil. $[\alpha]_D^{20} = -45.3$ ($c = 1.2$, CH₂Cl₂). IR (cm⁻¹) film: 3072, 2957, 1472, 1428, 1390, 1362, 1136, 1111, 1056, 992, 894, 824, 795, 739, 701. ¹H NMR (300

(44) Hua, D. H.; Venkataraman, S.; Ostrander, R. A.; Sinai, G. Z.; McCann, P. J.; Coulter, M. J.; Xu, M. R. *J. Org. Chem.* **1988**, *53*, 507–515.

MHz, CDCl₃): δ 7.75–7.62 (m, 4H), 7.46–7.32 (m, 6H), 6.22 (dd, $J = 10.9, 17.7$ Hz, 1H), 5.75 (t, $J = 3.4$ Hz, 1H), 4.94 (br d, $J = 17.7$ Hz, 1H), 4.76 (br d, $J = 10.9$ Hz, 1H), 3.72–3.65 (m, 2H); 2.20–2.09 (m, 3H), 1.93–1.79 (m, 1H), 1.30–1.13 (m+s, 4H), 1.06 (s, 9H), 0.90 (s, 3H). ¹³C NMR (75 MHz, CDCl₃): δ 139.6 (d), 136.1 (q), 136.0 (d), 135.9 (d), 134.0 (s), 133.7 (s), 130.4 (d), 129.6 (d), 127.7 (d), 127.6 (d), 109.8 (t), 64.0 (t), 46.4 (d), 31.8 (s), 31.6 (t), 29.1 (q), 27.3 (q), 27.0 (q), 23.8 (t), 19.3 (s). Anal. Calcd for C₂₇H₃₆OSi: C, 80.14; H, 8.97. Found: C, 80.26; H, 9.12.

Acknowledgment. We are deeply grateful to Dr. Philip Kraft, Givaudan Schweiz AG, Fragrance Research, Dübendorf,

Switzerland, for the skillful olfactory descriptions and the threshold values determinations. This work was supported by the Italian Ministero dell'Università e della Ricerca (MIUR) (COFIN grants) and by the University of Pavia (FAR grants). We thank CILEA for the allocation of computer time.

Supporting Information Available: Experimental procedures for compounds **8**, **9**, **10a**, **12**, **24**, and **27–34**; NMR spectra and computational data of new compounds; experimental details of the olfactory evaluation. This material is available free of charge via the Internet at <http://pubs.acs.org>.